# Application of Axisymmetric Analog for Calculating Heating in Three-Dimensional Flows

H. Harris Hamilton*
*NASA Langley Research Center, Hampton, Virginia*
Fred R. DeJarnette†
*North Carolina State University, Raleigh, North Carolina*
and
K. James Weilmuenster‡
*NASA Langley Research Center, Hampton, Virginia*

**A rapid, approximate method has been developed for calculating the heating rates on three-dimensional vehicles such as the Space Shuttle Orbiter and other advanced re-entry configurations. The method is based on the axisymmetric analog for three-dimensional boundary layers and uses information obtained from a three-dimensional inviscid flowfield solution to calculate inviscid surface streamlines along which approximate heating rates are calculated independent of other streamlines. Three-dimensional effects are included through the streamline metric coefficient. Boundary-layer edge properties are obtained from the inviscid flowfield solution by interpolation at a distance equal to the boundary-layer thickness away from the wall. This accounts, approximately, for the variable boundary-layer edge entropy. Using this method, heating calculations can be made along a typical streamline in a few seconds. This method is shown to accurately predict heating rates over the Shuttle Orbiter for both wind tunnel and flight conditions. A unique feature of the method is its ability to accurately predict heating rates on the Shuttle Orbiter wing.**

## Nomenclature

$b$ = wing span of Shuttle Orbiter
$C$ = wing chord
$h$ = streamline metric
$L$ = vehicle length
$M$ = Mach number
$p$ = pressure
$q$ = heating rate
$\bar{r},\theta,\phi$ = spherical coordinates
$Re$ = Reynolds number
$s,\beta,n$ = streamline coordinates (see Fig. 2)
$T$ = temperature
$u,v,w$ = velocity components in boundary layer
$u_r,u_z,u_\phi$ = velocity components in cylindrical coordinates
$u_{\bar{r}},u_\theta,u_\phi$ = velocity components in spherical coordinates
$V$ = total velocity
$x,y,z$ = Cartesian coordinates
$\bar{x},\bar{y},\bar{z}$ = local Cartesian coordinate system through stagnation point (see Fig. 4)
$z,r,\phi$ = cylindrical coordinates
$z^*$ = distance from wing leading edge
$Z_p$ = location of pole of spherical coordinate system
$\alpha$ = angle of attack
$\epsilon$ = cone angle relative to $\bar{z}$ axis (see Fig. 4)
$\tau$ = independent variable of integration in stagnation region, Eq. (4)

*Subscripts*

$b$ = body
$\infty$ = freestream

## Introduction

THE calculation of aerodynamic heating on advanced entry configurations is a challenging problem. Configurations of current interest are usually three-dimensional (nonaxisymmetric) bodies that can operate at large angles of attack during periods of peak heating. In many cases, it is possible to calculate heating in regions of attached flow using a "classical approach" where the outer inviscid flow is computed independent of the boundary layer and is used to provide edge conditions for a three-dimensional boundary-layer calculation near the surface.

A simple method of computing the boundary layer is to use the "axisymmetric analog" for three-dimensional boundary layers.[1] Following this approach, the general three-dimensional boundary-layer equations are written in a streamline coordinate system and the crossflow velocity is assumed to be zero. This reduces the three-dimensional boundary-layer equations to a form identical to those for axisymmetric flow, and allows any axisymmetric boundary-layer program to be used to compute the approximate three-dimensional heating along a streamline in regions where the small crossflow assumption is valid. By considering multiple streamline paths, an entire vehicle can be covered.

It has been shown that the crossflow in the boundary layer is small when the streamline curvature is small[2] or when the wall is highly cooled.[3] Thus, the small crossflow assumption is valid for many practical applications.

The most difficult part of applying this technique is computing the inviscid surface streamline paths and the metric coefficient associated with the spreading of the streamlines.

Presented as Paper 85-0245 at the AIAA 23rd Aerospace Sciences Meeting, Reno, NV, Jan. 14-17, 1985; received June 28, 1985; revision received Aug. 22, 1986. 

*Research Leader, Aerothermodynamics Branch, Space Systems Division. Member AIAA.
†Professor, Mechanical and Aerospace Engineering Department. Associate Fellow AIAA.
‡Aerospace Technologist, Aerothermodynamics Branch, Space Systems Division. Member AIAA.

Relatively simple methods have been developed for computing the streamline information from a known surface pressure distribution.[4,5] However, this approach has proven to be very difficult to apply except for relatively simple body shapes because of the difficulty in obtaining accurate surface pressure distributions. More success has been achieved by computing the streamline information from an inviscid velocity field obtained from a three-dimensional flowfield calculation.[6]

In the present paper, a new method is formulated for calculating the streamline paths and metric coefficient in three-dimensional flows using the inviscid velocity field. This method has proven to be very accurate and "robust." This new technique will be described and validated by comparing it with wind tunnel and previously published flight data for the Shuttle Orbiter. Comparisons will be made both along the windward-symmetry plane and off the symmetry plane, including the lower surface of the wing.

## Analysis

This section presents a discussion of the present approximate method for calculating heating rates in three-dimensional flows applicable to advanced re-entry vehicles such as shown in Fig. 1.

### Axisymmetric Analog

Following the approach of Cooke,[1] the general three-dimensional boundary-layer equations are first written in a streamline-oriented coordinate system $(s,\beta,n)$, where $s$ is measured along an inviscid surface streamline, $\beta$ is tangent to the surface and normal to the streamline direction, and $n$ is normal to the surface (see Fig. 2). If the crossflow velocity in the boundary layer is neglected, the boundary-layer equations reduce to the same form as for axisymmetric flow, provided that distance along a streamline is interpreted as distance along an equivalent axisymmetric body and that the metric coefficient $h$ that describes the spreading of streamlines is interpreted as the radius of an equivalent axisymmetric body. This greatly simplifies the boundary-layer problem and means that approximate three-dimensional heating rates can be computed along individual streamlines independent of other streamlines. However, a method must be devised for calculating the inviscid surface streamlines and metric coefficients.

### Inviscid Surface Streamlines and Metric Coefficient

Previous approaches for calculating the streamline and metric coefficients using a known surface pressure distribution[4] have proven to be unsatisfactory except for relatively simple cases such as sphere cones. The reason can be traced to the fact that the streamline metric calculations require second derivatives of the pressure. When these derivatives were calculated by finite-difference techniques, they proved to be inaccurate in many cases. A better approach is to use inviscid surface velocity components, when they are available, to perform the streamline and metric computations. This approach requires only first derivatives of the velocity components, which can be generated numerically with more accuracy than second derivatives.

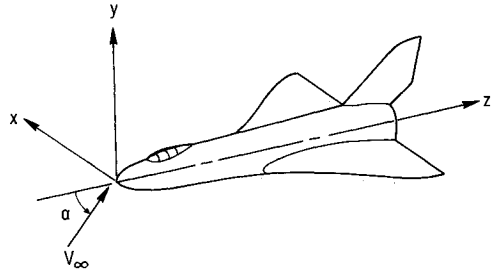


Fig. 1 Typical advanced re-entry vehicle.

The present method uses velocity components calculated by a three-dimensional inviscid flowfield solution, HALIS,[7] and a simple finite-difference technique to calculate their partial derivatives. The HALIS code provides the velocity components in spherical polar coordinates in the nose region and cylindrical coordinates in the region downstream of the nose (Fig. 3). However, for consistency, the surface geometry is described in cylindrical coordinates in both regions.

### Nose Region

In this region, the inviscid velocity components $(u_{\bar{r}},u_\theta,u_\phi)$ are given in spherical polar coordinates $(\bar{r},\theta,\phi)$, and the body geometry is described in cylindrical coordinates $(z,r,\phi)$ in the functional form

$$r_b = r_b(z,\phi) \tag{1}$$

Thus, the position of a streamline on the surface can be determined from the two independent variables $z$ and $\phi$. The inviscid velocity is used to calculate the successive positions of a streamline as it wraps around the body by integrating the ordinary differential equations[8]

$$\frac{D\phi}{D\tau} = u_\phi \tag{2}$$

$$\frac{Dz}{D\tau} = (-\sin\theta\, u_\theta + \cos\theta u_{\bar{r}})r_b \tag{3}$$

where $\tau$ is the variable of integration, which is related to the distance along a streamline $s$ by the relation

$$\frac{Ds}{D\tau} = Vr_b \tag{4}$$

The use of $\tau$ instead of $s$ as the integration variable eliminates some of the singularity problems at the stagnation and nose points. The streamline metric $h$ along a streamline

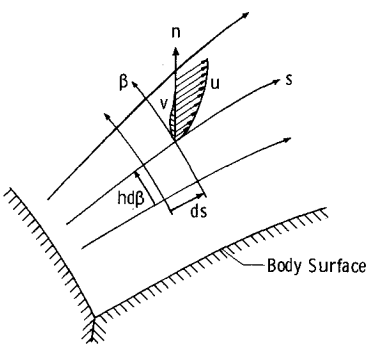


Fig. 2 Typical streamline and boundary-layer velocity profile.

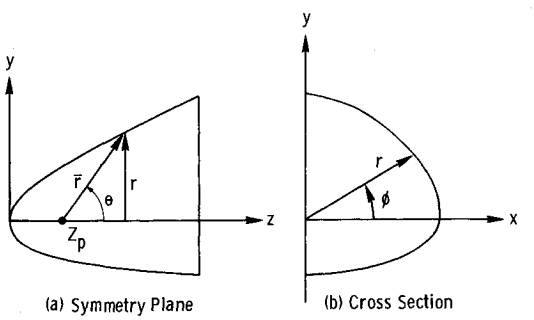


Fig. 3 Coordinate systems.

is determined by first integrating the equation

$$\frac{D}{D\tau}\ell n\left|\sin\theta\, u_\theta \frac{\partial\phi}{\partial\beta}\right| = \frac{\partial u_\phi}{\partial\phi} + \sin\theta\frac{\partial u_\theta}{\partial\theta} + \cos\theta\, u_\theta \qquad (5)$$

and then using the parameter $[\sin\theta u_\theta(\partial\phi/\partial\beta)]$ to calculate $h$ from the equation[8]

$$h = \left\{\bar{r}_b\left(-\sin\theta\, u_\theta \frac{\partial\phi}{\partial\beta}\right)\left[1+\left(\frac{\partial r_b}{\partial z}\right)^2+\left(\frac{1}{r_b}\frac{\partial r_b}{\partial\phi}\right)^2\right]^{1/2}\right\} \div V\left(\sin\theta - \frac{\partial r_b}{\partial z}\cos\theta\right) \qquad (6)$$

To establish the initial location of a streamline, first the stagnation point is located. Then the axis of a cone is established by the line connecting the stagnation point and the pole, or origin, of the spherical polar coordinate system (Fig. 4). A cone of half-angle $\epsilon$ is formed about this axis with its apex at the pole. The intersection of this cone with the body gives the curve along which the initial position of each streamline is specified. The location of each streamline on this curve is defined by the coordinate $\beta$, which is the circumferential angle about the cone axis. When the stagnation point lies on the nose point ($z=0$), the coordinate $\beta$ on the intersection of the cone with the body coincides with the circumferential angle $\phi$.

#### Region Downstream of Nose

In this region, both the inviscid velocity components $(u_z,u_r,u_\phi)$ and the body geometry are described in cylindrical coordinates $(z,r,\phi)$. The position of the streamline on the surface is determined by integrating the following differential equations:

$$\frac{D\phi}{Ds} = \frac{u_\phi}{r_b V} \qquad (7)$$

$$\frac{Dz}{Ds} = \frac{u_z}{V} \qquad (8)$$

where $s$ is distance along a streamline. The streamline metric $h$ along a streamline is determined by first integrating the equation

$$\frac{D}{Ds}\ell n\left(\frac{\partial\phi}{\partial\beta}\right) = \frac{1}{r_b V}\left(\frac{\partial u_\phi}{\partial\phi} - \frac{u_\phi}{u_z}\frac{\partial u_z}{\partial\phi} - \frac{u_\phi}{r_b}\frac{\partial r_b}{\partial\phi}\right) \qquad (9)$$

and then the parameter $\partial\phi/\partial\beta$ is used in the equation

$$h = r_b\frac{\partial\phi}{\partial\beta}\frac{u_z}{V}\left[1+\left(\frac{1}{r_b}\frac{\partial r_b}{\partial\phi}\right)^2+\left(\frac{\partial r_b}{\partial z}\right)^2\right] \qquad (10)$$

to finally calculate $h$.

#### Boundary-Layer Solution

With the axisymmetric analog, any axisymmetric boundary-layer method can be applied along a streamline to obtain a boundary-layer solution. In the present case, surface heating rates are the primary objective. Although these heating rates could be obtained from a finite-difference solution of the full axisymmetric boundary-layer equations, this is unnecessary because very accurate results can be obtained more easily from the approximate heating relations developed by Zoby et al.[9] These heating rate relations, valid for both laminar and turbulent flow, have been shown to yield results that compare favorably with more exact solutions for both wind tunnel and flight conditions,[10-12] with only a fraction of the computational effort required for a full boundary-layer solution. These heating rate equations are used exclusively in the present paper. Using this approach, heating rates along a typical streamline can be computed in approximately 15–20 s on a CDC CYBER 730 computer.

#### Inviscid Flowfield Solution and Boundary-Layer Edge Properties

The method presented in the current paper for computing heating in three-dimensional flows requires the three-dimensional velocity field over the vehicle in order to calculate the necessary streamline paths and metric coefficients. The only accurate method of obtaining this information is from a three-dimensional inviscid flowfield solution. While many methods are available, the only method known to the present authors that can be applied to compute the inviscid flowfield over a complete vehicle (including the wings) such as the Shuttle Orbiter is the HALIS code developed by Weilmuenster and Hamilton.[7] This method has been shown to provide accurate flowfield results over the Shuttle Orbiter at angles of attack as high as 45 deg (see Ref. 13).

The HALIS code is a time-dependent solution of the Euler equations that is programmed to run on a vector-processing computer. All of the heating rate calculations presented in the present paper use the HALIS inviscid flowfield solutions. A typical inviscid solution for the Shuttle Orbiter requires approximately 90,000 grid points and 75 min of computing time on the CDC CYBER 203 computer.

Boundary-layer edge properties are obtained by interpolating in the inviscid flowfield at a distance equal to the boundary-layer thickness away from the wall. To accomplish this, an initial assumption is made for the boundary-layer edge properties (equal to the wall values), and then the solution is iterated until the assumed values for the edge properties are equal to the calculated values. This process usually takes two or three iterations to converge and can be carried out at each step as the heating calculations are being made. A similar procedure has been used previously with good results for both axisymmetric[9] and three-dimensional[14] flow. Edge properties determined in this manner account, approximately, for the variable boundary-layer edge entropy effect that has been shown to be of great importance for high-velocity entry conditions.

## Results and Discussion

A relatively simple approximate method has been described for computing the heating on the windward side of three-dimensional vehicles such as the Space Shuttle Orbiter. This method is based on the axisymmetric analog and can be applied to any vehicle for which the inviscid flowfield can be computed. In this section, heating rates on the Shuttle Orbiter calculated by this method will be compared with experimental data for both wind tunnel and flight conditions.

#### Wind Tunnel Comparisons

Calculated heating rates along the windward-symmetry plane of the Shuttle Orbiter are compared with wind tunnel

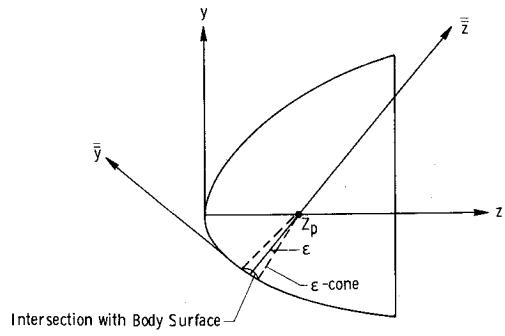


**Fig. 4 Geometry of initial $\epsilon$ cone.**

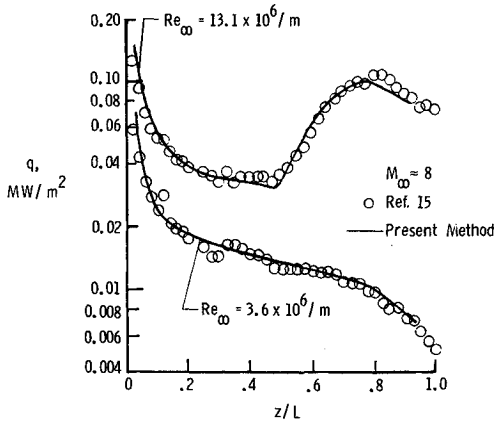


**Fig. 5 Heating distribution along wind symmetry plane of 0.0175-scale Shuttle Orbiter for $\alpha = 35$ deg.**

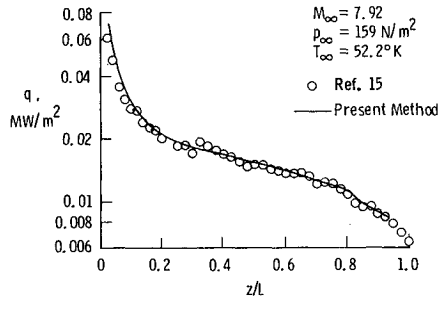


**Fig. 6 Heating distribution along windward-symmetry plane of 0.0175-scale Shuttle Orbiter for $\alpha = 40$ deg, $Re_\infty = 3.6 \times 1.0^6$/m.**

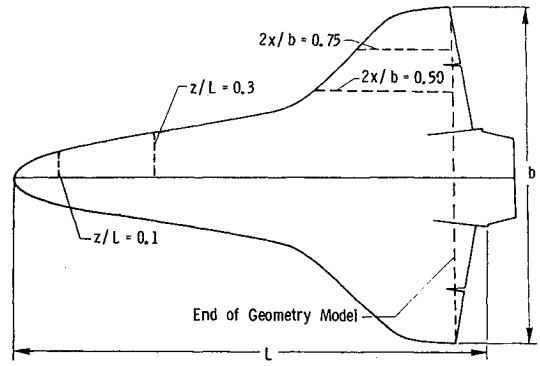


**Fig. 7 Location of off-symmetry plane heating comparisons for 0.0175-scale Shuttle model.**

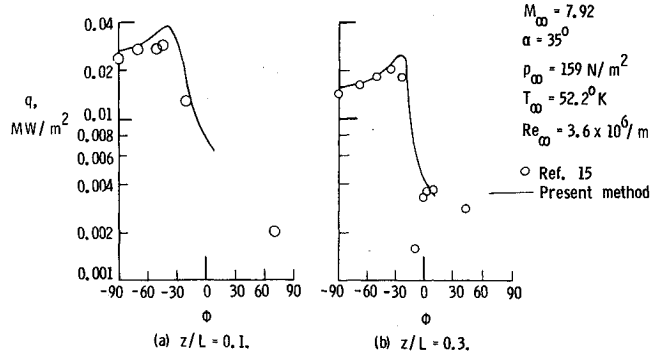


**Fig. 8 Circumferential distribution of heating on 0.0175-scale Shuttle Orbiter.**

data, measured on an 0.0175-scale ($L = 0.576$ m) model,[15] in Figs. 5 and 6. These data were obtained at a freestream Mach number of approximately 8 and cover an angle-of-attack range of 35 to 40 deg and a freestream Reynolds number range of $3.6 \times 10^6$/m to $13.1 \times 10^6$/m.

Results for a 35 deg angle of attack are shown in Fig. 5. At a freestream Reynolds number of $3.6 \times 10^6$/m, the flow along the windward symmetry plane is completely laminar, and the calculations are in excellent agreement with the experimental data. At the higher Reynolds number of $13.1 \times 10^6$/m, transition starts near $z/L = 0.47$ and the flow becomes fully turbulent near $z/L = 0.8$. The calculated turbulent results are in very good agreement with the experimental data from this point downstream. There is no mechanism in the present code for "triggering" transition automatically; thus, the beginning and end of transition must be specified. The distribution of heating in the transition region is based on an exponential distribution function similar to that used by Dhawan and Narasimha.[16] The results for heating in the transition region for this case are excellent.

In Fig. 6, comparisons are shown for heating along the windward symmetry plane for a 40 deg angle of attack and a freestream Reynolds number of $3.6 \times 10^6$/m. As was the case at the lower angle of attack at this Reynolds number, the flow is laminar and the calculated results are in excellent agreement with the experimental data.

As has been demonstrated, the present method is capable of predicting the heating along the windward-symmetry plane of vehicles such as the Shuttle Orbiter, agreeing well with the experimental data. Similar results can be obtained for the heating along the windward-symmetry plane using other much simpler methods[11,12,17] which require much less computational effort. However, the real utility of the present method is its ability to compute the heating off the symmetry plane. To demonstrate this capability, comparisons will be presented for heating on the lower surface of the Shuttle Orbiter at the locations marked in Fig. 7.

First, comparisons of the lateral distributions of heating on the lower surface of the fuselage are presented at two axial stations ($z/L = 0.1$ and 0.3) in Fig. 8. These results were obtained at an angle of attack of 35 deg for the same flow conditions as the data in Fig. 6. The heating rate is presented as a function of circumferential angle $\phi$ starting in the windward-symmetry plane ($\phi = -\pi/2$) and proceeding toward the leeward symmetry plane ($\phi = \pi/2$). Calculations are not shown for values of $\phi$ greater than 10 deg because the flow on the leeward side of the vehicle is viscous-dominated at this angle of attack, and the present method is unable to account for this effect. The calculated results are in reasonably good agreement with the experimental data at each axial station, although the experimental data are slightly overpredicted near the peak at $z/L = 0.1$ (see Fig. 8a).

A comparison of calculated and measured heating rates on the wing at values of $2x/b = 0.50$ and 0.75 are shown in Fig. 9. These results are presented as local heating rate vs nondimensional distance along the wing chord $z^*/C$. The comparisons at the "midwing" location, $2x/b = 0.50$, are presented in Fig. 9a. There is some scatter in the data, and the calculated results are slightly higher for $z^*/C = 0.2$ to 0.3, but the overall comparisons are very good. Even the high heating on the wing leading edge is predicted with reasonable accuracy.

Comparisons at the more outboard wing location, $2x/b = 0.75$, are presented in Fig. 9b. Again, the calculated heating rate is in very good agreement with the measured heating rate except near $z^*/C = 0.7$ to 0.8, where the measured heating is much lower. The much lower heating in this region and at $z^*/C = 0.2$ to 0.3 for the "midwing" location in Fig. 9a is probably the result of the "streak heating" phenomenon that has been observed by other investigators.[18]

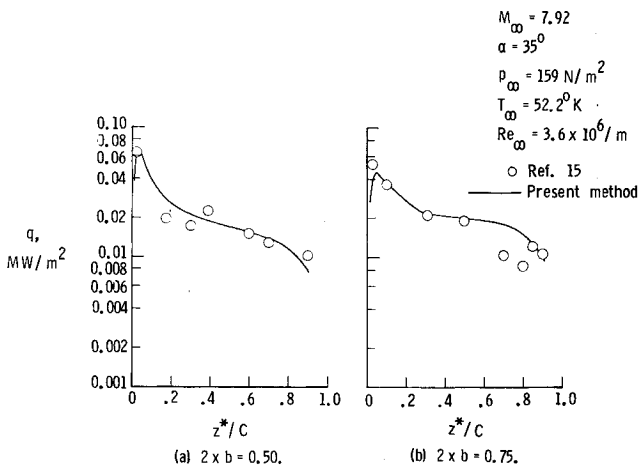


**Fig. 9 Streamwise distribution of heating on wing of 0.0175-scale Shuttle Orbiter.**

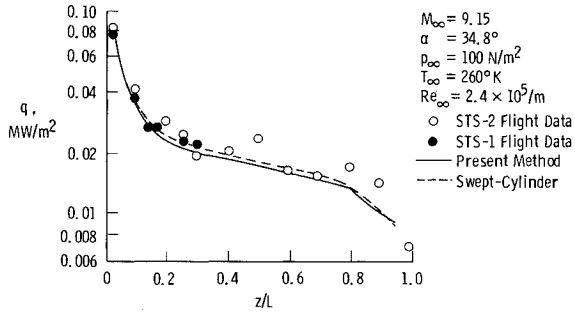


**Fig. 10 Heating distribution along windward-symmetry plane of full-scale Shuttle Orbiter.**

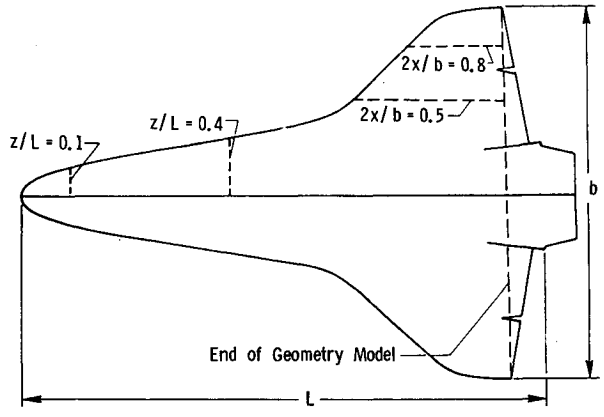


**Fig. 11 Location of off-symmetry plane heating comparisons for full-scale Shuttle Orbiter.**

More detailed inviscid solutions would be needed before this phenomenon could be investigated any further using the present theoretical method. There is some indication in the present inviscid results[18] which indicates a disturbance propagating across the wing from the intersection of the wing shock and bow shock, but these disturbances do not appear to affect the calculated heating rates.

### Flight Data Comparisons

Next, comparisons are made between calculations and experimental data obtained in flight. The case considered is for STS-2. The flight conditions are as follows: $M_\infty = 9.15$, $\alpha = 34.8$ deg, $p_\infty = 100$ N/m$^2$, and $T_\infty = 260$ K. The analysis is performed for an ideal gas with $\gamma = 1.4$. Comparisons of heating along the windward-symmetry plane for this case are shown in Fig. 10. Also presented in the figure are some laminar heating rates from STS-1 for the same flight conditions. Although there is considerable scatter in the experimental data, the present calculations are in reasonably good agreement. Heating rates calculated by a swept-cylinder method[17] that has been shown to give good results over a wide range of flight conditions are also shown in the figure. The heating rates calculated by the present method are also in very good agreement with these results. The primary advantage of the present method over most other methods is that it can be easily used to make calculations off the windward-symmetry plane. Comparisons of calculated heating rates with the flight data off the windward-symmetry plane have been made at all of the locations marked in Fig. 11.

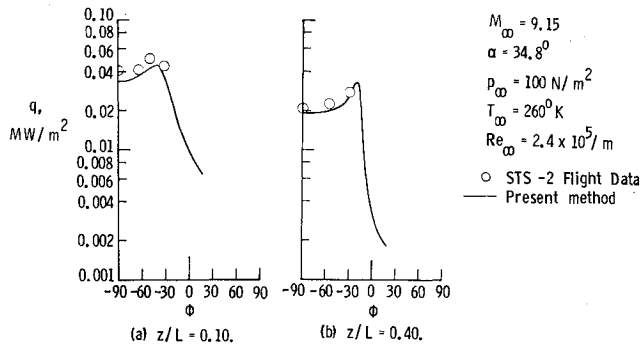


**Fig. 12 Circumferential distribution of heating on full-scale Shuttle Orbiter.**

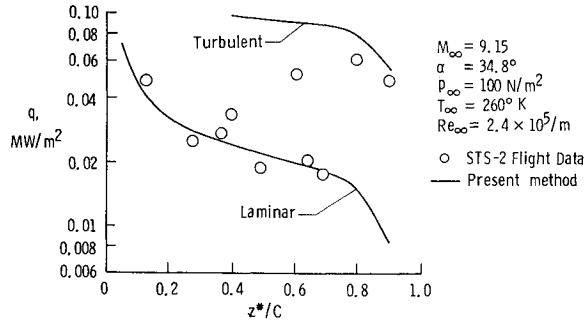


**Fig. 13 Streamwise distribution of heating on wing of full-scale Shuttle Orbiter at $2x/b = 0.5$.**

First, circumferential distributions of heating are presented at two axial stations ($z/L = 0.1$ and 0.4) on the fuselage of the Shuttle Orbiter in Fig. 12. The present calculated results are in very good agreement with the data.

A comparison of calculated heating with flight data for the "midwing" location ($2x/b = 0.5$) is presented in Fig. 13. Two theoretical curves are shown, one for laminar flow and one for turbulent flow. The turbulent calculations were made by starting transition at $z/L = 0.2$. At first glance the flight data appear to behave very strangely, first being laminar, then transitional, then laminar, then transitional, then laminar again, and finally being fully turbulent near the trailing edge of the wing. This behavior is quite easily explained when it is realized that the flow at different chord locations on the wing has traveled along different streamlines. This can be seen from the inviscid surface streamline pattern for this case, shown in Fig. 14. Thus, flow along one streamline can be transitional or even turbulent while the flow on adjacent streamlines remains laminar. In fact, this behavior fits the transition pattern observed for this case by Hartung and Throckmorton,[19] which is shown in the transition front locations in Fig. 15.

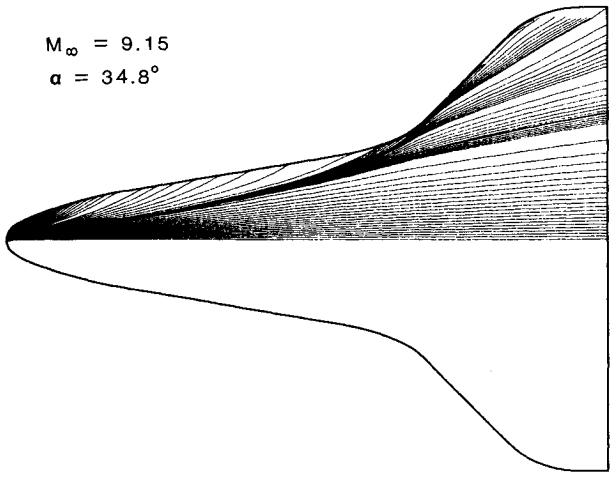


**Fig. 14 Streamline pattern on full-scale Shuttle Orbiter.**

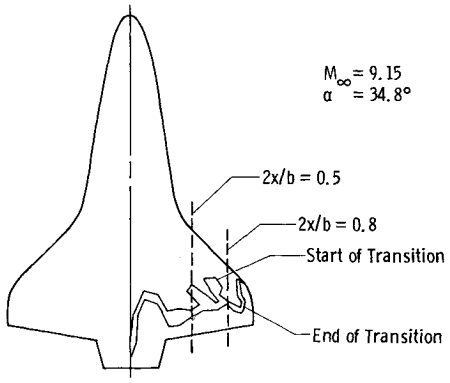


**Fig. 15 Transition front on Shuttle Orbiter wing from STS-2 flight.**

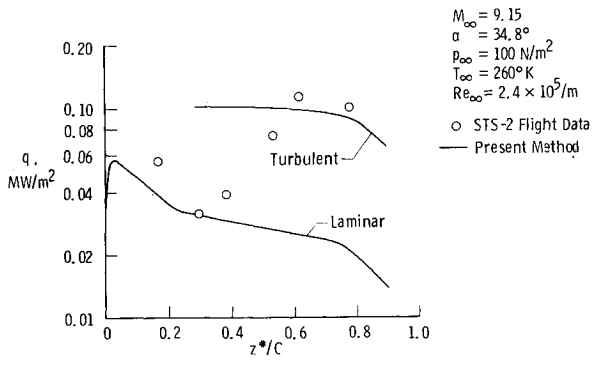


**Fig. 16 Streamwise distribution of heating on wing of full-scale Shuttle Orbiter at $2x/b = 0.8$.**

The heating at the more outboard location on the wing ($2x/b = 0.8$) is presented in Fig. 16. The heating pattern for this case is typical of that expected for a flow undergoing transition. The flow near the leading edge of the wing is laminar, then undergoes transition and finally becomes fully turbulent near the trailing edge. The calculated heating in the laminar and turbulent regions of the flow is in reasonably good agreement with the flight data.

## Concluding Remarks

A rapid, approximate method has been developed for calculating the heating rates on three-dimensional vehicles such as the Space Shuttle Orbiter and other advanced reentry configurations. The method is based on the axisymmetric analog for three-dimensional boundary layers. It uses information obtained from a three-dimensional inviscid flowfield solution such as HALIS to calculate inviscid surface streamlines along which approximate heating rates are calculated independent of other streamlines. Three-dimensional effects are included through the metric coefficient that describes the divergence or convergence of streamlines. Boundary-layer edge properties are obtained from the inviscid flowfield solution by interpolating in the inviscid flowfield at a distance equal to the boundary-layer thickness away from the wall. This accounts, approximately, for the variable boundary-layer edge entropy. Using this method, heating calculations along a typical streamline can be made in a few seconds. This method has been shown to accurately predict both laminar and turbulent heating rates on the Shuttle Orbiter for both wind tunnel and flight conditions.

One of the unique features of the present method is its ability to compute heating rates off the windward-symmetry plane for complex shapes such as the Shuttle Orbiter. This ability has been demonstrated in the present paper by using the method to predict heating rates on both the orbiter fuselage and wing. In both cases, the predicted heating rates were in good agreement with the experimental data. To the authors' knowledge, this is the only detailed method that has been demonstrated to accurately predict heating rates on the wing of a vehicle as complex as the Shuttle Orbiter.

## References

[1]Cooke, J. C., "An Axially Symmetric Analogue for General Three-Dimensional Boundary Layers," R&M 3200, British ARC, 1961.

[2]Hayes, W.D., "The Three-Dimensional Boundary Layer," NAVORD Rept. 1313 (NOTS 384), U.S. Naval Ordnance Test Station, Inyoken, China Lake, CA, May 1951.

[3]Vaglio-Laurin, R., "Laminar Heat Transfer on Three-Dimensional Blunt Nosed Bodies in Hypersonic Flow," *ARS Journal,* Vol. 29, Feb. 1959, pp. 123-129.

[4]DeJarnette, F. R. and Hamilton, H.H., "Inviscid Surface Streamlines and Heat Transfer on Shuttle-Type Configurations," *Journal of Spacecraft and Rockets,* Vol. 10, May 1973, pp. 314-321.

[5]DeJarnette, F. R., "Aerodynamic Heating on Complex Configurations," AIAA Paper 79-0891, 1979.

[6]Hamilton, H. H. II, "Calculation of Laminar Heating Rates on Three-Dimensional Configurations Using the Axisymmetric Analogue," NASA TP 1698, Sept. 1980.

[7]Weilmuenster, K. and Hamilton, H.H. II, "High Angle of Attack Inviscid Flow Calculations Over Shuttle-Like Vehicles With Comparisons to Experimental Data," NASA TP 2103, 1982.

[8]Hamilton, H. H., DeJarnette, F. R., and Weilmuenster, K. J., "Application of Axisymmetric Analogue for Calculating Heating in Three-Dimensional Flows," AIAA Paper 85-0245, Jan. 1985.

[9]Zoby, E. V., Moss, J. N., and Sutton, K., "Approximate Convective Heating Equations for Hypersonic Flows," *Journal of Spacecraft and Rockets,* Vol. 18, Jan. 1981, pp. 64-70.

[10]Zoby, E. V., "Approximate Heating Analysis for the Windward Symmetry Plane of Shuttle-Like Bodies at Large Angle of Attack," *Progress in Astronautics and Aeronautics,* Vol. 82, edited by T. E. Horton, AIAA, New York, 1982, pp. 229-247.

[11]Zoby, E. V., "Comparisons of STS-1 Experimental and Predicted Heating Rates," *Journal of Spacecraft and Rockets,* Vol. 20, May-June 1983, pp. 214-218.

[12]Zoby, E. V., "Analysis of STS-2 Experimental Heating Rates and Transition Data," *Journal of Spacecraft and Rockets,* Vol. 20, May-June 1983, pp. 232-237.

[13]Weilmuenster, K., "High Angle of Attack Inviscid Flow Calculations Over a Shuttle-Like Vehicle With Comparisons to Flight Data," AIAA Paper 83-1798, July 1983.

[14]Rakich, J. V. and Lanfranco, M. J., "Numerical Computation of Space Shuttle Laminar Heating and Surface Streamlines," *Journal of Spacecraft and Rockets,* Vol. 14, May 1977, pp. 265-272.

[15]Herrera, B. J., "Results From a Convective Heat Transfer Rate Distribution Test on a 0.0175 Scale Model (22-0) of the Rockwell International Vehicle 4 Space Shuttle Configuration in the AEDC-VKF Tunnel B (OH49B)," Vol. 1, NASA CR-147626, Vol. 2, NASA CR-147627, 1976.

[16]Dhawan, S. and Narasimha, R., "Some Properties of Boundary Layer Flow During Transition from Laminar to Turbulent Motion," *Journal of Fluid Mechanics,* Vol. 3, April 1958, pp. 418-436.

[17]Hamilton, H. H. II, "Approximate Method of Predicting Heating on the Windward Side of Space Shuttle Orbiter and Comparisons with Flight Data," *Progress in Astronautics and Aeronautics,* Vol. 85, edited by P. E. Bauer and H. E. Collicot, AIAA, New York, 1983, pp. 21-53.

[18]Throckmorton, D. A. and Hartung, L. C., "Analysis of Entry Aerodynamic Heat Transfer Data for the Orbiter Wing Lower Surface," AIAA Paper 84-0227, Jan. 1984.

[19]Hartung, L. C. and Throckmorton, D. A., "Computer Graphic Visualization of Orbiter Lower Surface Boundary-Layer Transition," AIAA Paper 84-0228, Jan. 1984.